表1　コーヒーと糖尿病（コホート研究のまとめ）

国（報告年）	対象人数	糖尿病の診断	比較（1日杯数）	相対危険（95%信頼区間）
オランダ (2002)	男女1万7111名	自己申告	7+と≦2杯	0.50 (0.35-0.72)
フィンランド (2003)	男女1万9518名	薬剤処方記録	7+と＜2杯	0.92 (0.73-1.16)
米国 (2003)	ピマ族824名	WHO1985年	3+と0杯	1.01 (0.82-1.26)
スウェーデン (2004)	女性 1361名	退院記録ほか	7+と≦2杯	0.48 (0.22-1.06)
フィンランド (2004)	男女1万4629名	退院記録と薬剤処方記録	10+と≦2杯	0.39 (0.24-0.64)
米国 (2004)	男性4万1934名	自己申告	6+と0杯	0.46 (0.26-0.82)
	女性8万4276名			0.71 (0.56-0.89)
フィンランド (2004)	双子1万652名	退院記録と薬剤処方記録	7+と≦2杯	0.65 (0.44-0.96)

表2　コーヒーと耐糖能異常

国（報告年）	対象人数	比較（1日杯数）		相対危険（95%信頼区間）
スウェーデン(2004)[1] 断面研究	男性3,128名	5+と≦2杯	糖尿病*1	0.45 (0.22-0.92)
			IGT	0.63 (0.41-0.97)
	女性4,821名		糖尿病	0.27 (0.11-0.66)
			IGT	0.47 (0.29-0.76)
日本 (2004)[2] 断面研究	男性3,224名	5+と0杯	糖尿病*2	0.8 (0.5-1.3)
			IGT	0.6 (0.4-0.8)
			IFG	0.9 (0.6-1.4)
オランダ (2004)[3] 縦断研究	男女1,312名	7+と≦2杯	糖尿病*2	0.69 (0.31-1.51)
			IGT	0.37 (0.16-0.84)
			IFG	1.35 (0.80-2.27)

*1：1985年WHO診断基準，*2：1998年WHO診断基準
IGT : impaired glucose tolerance（耐糖能障害），IFG : impaired fasting glycemia（空腹時高血糖）

〈参考文献〉
1）Agardh EE, Carlsson S, Ahlbom A et al : Coffee consumption, type 2 diabetes and impaired glucose tolerance in Swedish men and women. J Intern Med 255 : 645-652, 2004
2）Yamaji T, Mizoue T, Tabata S et al : Coffee consumption and glucose tolerance status in middle-aged Japanese men. Diabetologia 47 : 2145-2151, 2004
3）van Dam RM, Dekker JM, Nijpels G et al : Coffee consumption and incidence of impaired fasting glucose, impaired glucose tolerance, and type 2 diabetes: The Hoorn Study. Diabetologia 47 : 2152-2159, 2004

特集：コーヒー
Coffee

コーヒーと生活習慣病予防

九州大学大学院医学系研究科
予防医学分野
古野 純典

はじめに

従来、コーヒーは身体に悪いとの印象が一般的にあったが、むしろコーヒーが健康に良いことがいくつか明らかになりつつある。1980年代の北欧の疫学研究では、コーヒー飲用が虚血性心疾患のリスクを高めることが指摘されている。これは、北欧で伝統的に飲用されていた非フィルターの煮沸コーヒーに含まれるカフェストールやカヘオールなどの油性成分ディテルペンが動脈硬化を促進するLDLコレステロールを上昇させるためであることがわかっている。現在は北欧でもフィルター・コーヒーが広まり、最近の研究ではコーヒーによる虚血性心疾患リスクの高まりは認められていない。一般に飲用されているフィルター・コーヒーやインスタント・コーヒーにはコレステロール上昇作用を持つディテルペンはほとんど含まれていない。本稿では、生活習慣病予防の観点からその効果がほぼ間違いないと考えられるコーヒーの肝臓病予防効果と糖尿病予防効果について解説する。

コーヒーと肝臓病

1）飲酒による肝障害

過度の飲酒は、初期には血清γ-GTPを上昇させ、長期にわたると肝臓に脂肪沈着をきたす（脂肪肝）。慢性的にはアルコール性肝炎や肝硬変をもたらすことになる。アルコール性肝炎の状態では、肝細胞が破壊され、細胞内の酵素であるGOT（AST）やGPT（ALT）などが血中に逸脱するので、血清のGOTやGPTが上昇する。血清GOTやGPTが高くなく、γ-GTPだけが高値の場合は肝障害の程度はきわめて軽度である。これらの血清酵素の値は測定方法で異なるが、一般的にはGOTとGPTは40U／L以下、γ-GTPは50U／L以下とされている。

γ-GTPは、ヒトでは腎臓で活性が最も高く、次いで膵臓、肝臓などで活性が高い。血清γ-GTPは肝・胆道系の病気で高値を示し、肝・胆道系疾患のスクリーニング検査として広く用いられている。特に、アルコール性肝障害の場合に著しく上昇し、禁酒によ

りすみやかに改善するので、過剰飲酒の指標として用いられる。血清γ-GTPは肥満している人でも上昇するが、脂肪肝の前兆と考えられる。

2）コーヒーと肝機能血液検査値

健常人の血清γ-GTPに影響する要因としては飲酒と肥満以外にはほとんど知られていなかったが、1980年代後半から1990年代にかけてノルウェーとイタリアの疫学研究において、血清γ-GTPがコーヒーの摂取量（杯数）と負に相関していることが初めて指摘された（表1）。これらの結果は予想外のことで、どのような機序でコーヒー飲用者においてγ-GTPが低値であるのかはまったく不明である。ノルウェーの1つの研究は縦断的研究であるが、他の3つは、現在の血清γ-GTPの値が現在のコーヒー飲用習慣とどのように関係しているかを見ている断面的研究である。断面的疫学研究の場合には、病気のために調べている要因が変化している可能性が問題になる。すなわち、コーヒーとγ-GTPの負の関係は、肝臓が悪くてコーヒーを飲まなくなったためだとの解釈もできる。

表1 コーヒー飲用と肝機能血液検査値

国（報告年）	方法	対象人数	主要な結果
ノルウェー（1986）	横断研究	男 1579 女 1654	杯数が多いとγ-GTP 低値
ノルウェー（1990）	横断研究	男 10942 女 10840	杯数が多いとγ-GTP 低値
イタリア（1993）	横断研究	男女 2240	杯数が多いとγ-GTP，ALT 低値
ノルウェー（1994）	縦断研究	男 1171 女 1267	煮沸コーヒー摂取増加女性でγ-GTP 低下
日本（1994）	横断研究	男 2494	杯数が多いとγ-GTP 低値
米国（1995）	横断研究	バス運転手 343	カフェイン摂取量が多いとγ-GTP 低値
フィンランド（1997）	横断研究	男女 6010	杯数が多いとγ-GTP 低値
日本（1998）	横断研究	男 7398 女 5289	杯数が多いとγ-GTP，AST，ALT 低値
日本（1999）	横断研究	男 7637	杯数が多いとγ-GTP 低値
日本（2000）	横断研究	男 1353	杯数が多いとγ-GTP 低値
日本（2000）	縦断研究	男 1014	杯数増加者でγ-GTP 低下
日本（2000）	縦断研究	男 1221	杯数増加者でAST，ALT 低下
日本（2001）	横断研究	男 7313	1日杯数が多いとAST，ALT 低値
米国（2005）	横断研究	男女 5944	1日杯数が多いとALT 低値

ALT：アラニン・アミノトランスフェラーゼ（別名 GPT）
AST：アスパルテート・アミノトランスフェラーゼ（別名 GOT）

その後の日本、米国およびフィンランドにおける研究でもコーヒー飲用者で血清γ-GTPが低値であることが確認されている。私どもの最初の研究は約2500名の男性自衛官を対象とした断面的研究であるが、1日あたりに飲用するコーヒー杯数別の血清γ-GTPの幾何平均値は、0杯で31U／L、1～2杯で26U／L、3～4杯で25U／L、5杯以上で22U／Lであった。長野県中部公衆医学研究所が実施した住民健診と職域健診の受診者を対象とした研究においても同様の結果であり、約7000人からなるその後の自衛官の研究でもコーヒーとγ-GTPの負の相関が確認された。自衛官の研究ではインスタント・コーヒーとレギュラー・コーヒーを区別してγ-GTPとの関係を検討したが、両者に大きな違いは見られなかった。最近では、大阪府の企業従業員の研究で同様の結果が報告されている。緑茶はコーヒー同様カフェイ

ンの主要摂取源であるが、緑茶飲用は血清γ-GTPの値と関係がなかった。カフェイン以外のコーヒー成分が血清γ-GTP低下作用を有していると考えられる。

アルコールと肥満は血清γ-GTP値を上昇させる重要な要因であるので、γ-GTPに対するコーヒー飲用とこれらの要因との交互作用は当然興味がもたれるところである。自衛官の研究では、このことを詳細に検討した。アルコール摂取量が多いほどγ-GTP値はほぼ直線的に増加するが、コーヒーを毎日飲んでいる者では増加のしかたが緩やかであった（図1）。一方、コーヒー飲用の有無にかかわらず、肥満度が高いほどγ-GTPは高値であった。これらの結果はコーヒー飲用がアルコールによるγ-GTPの上昇を抑制することを強く示唆するものである。長野県中部公衆医学研究所が実施した住民健診と職域健診の受診者を対象とした研究においても、コーヒー飲用とアルコール性肝障害の予防的関連性を確認した。また、その後の約7000人からなる自衛官の研究でも同じような結果が得られた。

肝障害が進むとAST（GOT）やALT（GPT）の血液検査値も高くなる。コーヒー飲用杯数が多い人ではASTやALTの検査値も低いことがイタリア、日本および米国の研究で報告されている。ちなみに、肝障害の指標としてはASTよりALTの方がより有用とされている。

3）コーヒーと肝硬変

長期にわたる大量飲酒は肝硬変の原因であるが、米国とイタリアの5つの研究でコーヒーが肝硬変に予防的であることが観察されて

図1

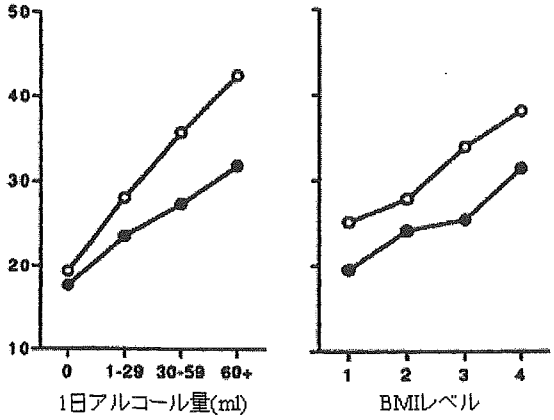

飲酒によるγ-GTPの増加はコーヒー非飲用者（○）に比べ毎日飲用者（●）で緩やかである。肥満によるγ-GTPの増加にはコーヒー飲用の有無で違いはない。

表2 コーヒー飲用と肝硬変

国（報告年）	調査方法	対象人数	1日杯数	相対危険度
米国（1992）	コホート研究	男女約13万（肝硬変89）	≥4杯	0.2（標記なし）[注]
イタリア（1994）	症例対照研究	症例115名 対照167名	≥2杯	0.7（0.4-1.4）
米国（2001）	症例対照研究	症例274名 対照458名	≥4杯	0.16（0.05-0.50）
イタリア（2002）	症例対照研究	症例101名 対照1,538名	≥3杯	0.29（標記なし）
イタリア（2003）	コホート研究	男女約5万（肝硬変死亡53）	2杯当たり	0.6（0.5-0.8）

相対危険度は、表に示したコーヒー1日杯数の非飲用に対する危険度。
注）アルコール性肝硬変による入院

いる（表2）。米国の医療保険加入者を対象にした大規模コホート研究では、コーヒー摂取量が多い者ほどアルコール性肝硬変による入院の危険度およびアルコール性肝硬変による死亡危険度が低いことが指摘されている。非飲酒者に比べ毎日6杯（アルコール量60～90 ml）以上飲酒している者のアルコール性肝硬変による入院の危険度は、コーヒーを飲まない人で84倍も高率であったが、コーヒーを毎日飲んでいる人では16倍程度であった。イタリアの症例対照研究でも、コーヒーがアルコールと関連した肝硬変危険度の高まりを抑制することが報告されている。これら2つの研究はアルコール性肝硬変に対して特に予防的であることが示されているが、別の研究ではアルコールと関係しない肝硬変（B型あるいはC型肝炎ウイルスに起因する肝硬変）についても予防的であると指摘されている。

4）コーヒーと肝臓がん予防

コーヒーが肝臓がんに予防的であることは、2002年にイタリアとギリシャの症例対照研究ではじめて報告された。2005年には、イタリアで別の症例対照研究とわが国で2つのコホート研究の結果が報告されたが、いずれもコーヒーの肝臓がん予防効果を示す結果である（表3）。これら5つの研究のいずれもコーヒー摂取量が多い人ほど肝臓がん危険度がより低くなっている。また、2つの研究ではアルコール摂取量が多い人、B型肝炎ウイルス感染者、C型肝炎ウイルス感染者でも、コーヒー飲用により肝臓がん危険度の一様な低下が観察されている。

コーヒーと糖尿病

1）糖尿病に関するコホート研究（追跡調査研究）

肥満防止と運動が2型糖尿病の予防に重要な要因であるが、ごく最近、コーヒー飲用が2型糖尿病に予防的であることがわかってきた。コーヒーが2型糖尿病に予防的であることは、オランダのコホート研究で2002年にはじめて報告された。その後のフィンランドと米国ピマ・インディアンのコホート研究ではコーヒーと糖尿病の予防的な関係ははっきりしなかったが、2004年に相次いで発表されたスウェーデン、フィンランドおよび米国における4つのコホート研究からは、い

表3　コーヒー飲用と肝臓がん

国（報告年）	調査方法	対象人数	1日杯数	相対危険度（95%信頼区間）
ギリシャ（2002）	症例対照研究	症例333名　対照360名	≥3	0.6（0.4-1.1）
イタリア（2002）	症例対照研究	症例501名　対照1552名	≥3	0.5（0.4-0.7）
イタリア（2005）	症例対照研究	症例250名　対照500名	≥5	0.3（0.1-0.7）
日本（2005）	コホート研究	男女約9万（肝がんり患334例）	≥5	0.24（0.08-0.77）
日本（2005）	コホート研究	男女約6万（肝がんり患117例）	≥1	0.58（0.36-0.96）

相対危険度は、表に示したコーヒー1日杯数の非飲用に対する危険度。

ずれもコーヒーが2型糖尿病の発症に予防的であることが示された（表4）。フィンランドにおける最初の研究では糖尿病の薬剤処方を受け始めた者を糖尿病の新規発症者としているので、糖尿病の確認が不十分であると思われる。また、ピマ・インディアンは糖尿病が多発することで有名な集団であり、コーヒーの影響を調べにくい集団であると思われる。

2）耐糖能に関する研究

インスリン抵抗性を基盤とする2型糖尿病は、前糖尿病状態である耐糖能障害が進展して起こるものである。したがって、コーヒーが耐糖能障害（IGT）に対しても予防的であるか否かは、コーヒーの糖尿病予防の機序を考える上で興味深い。耐糖能は、一般に75g経口ブドウ糖負荷試験によって判定される。コーヒーと耐糖能との関係を見た研究は世界で3つだけ報告されている（表5）。3つの研究のいずれでもコーヒーが耐糖能障害（IGT）に予防的であることが示されている。空腹時血糖異常（IFG）が定義されたWHO1998年診断基準を用いた2つの研究では、コーヒーと空腹時血糖異常（IFG）との関係ははっきりしない。コーヒーは、食

表4 コーヒーと糖尿病（コホート研究のまとめ）

国（報告年）	対象人数	糖尿病の診断	比較（1日杯数）	相対危険（95%信頼区間）
オランダ（2002）	男女 17111 名	自己申告	7+と≦2 杯	0.50（0.35-0.72）
フィンランド（2003）	男女 19518 名	薬剤処方記録	7+と<2 杯	0.92（0.73-1.16）
米国（2003）	ピマ族 824 名	WHO1985 年	3+と 0 杯	1.01（0.82-1.26）
スウェーデン（2004）	女性 1361 名	退院記録・他	7+と≦2 杯	0.48（0.22-1.06）
フィンランド（2004）	男女 14629 名	退院記録と薬剤処方記録	10+と≦2 杯	0.39（0.24-0.64）
米国（2004）	男性 41934 名	自己申告	6+と 0 杯	0.46（0.26-0.82）
	女性 84276 名			0.71（0.56-0.89）
フィンランド（2004）	双子 10652 名	退院記録と薬剤処方記録	7+と≦2 杯	0.65（0.44-0.96）

表5 コーヒーと耐糖能異常

国（報告年）	対象人数	比較（1日杯数）		相対危険（95%信頼区間）
スウェーデン（2004）	男性 3128 名	5+と≦2 杯	糖尿病[注1)]	0.45（0.22-0.92）
断面研究			IGT	0.63（0.41-0.97）
	女性 4821 名		糖尿病	0.27（0.11-0.66）
			IGT	0.47（0.29-0.76）
日本（2004）	男性 3224 名	5+と 0 杯	糖尿病[注2)]	0.8（0.5-1.3）
断面研究			IGT	0.6（0.4-0.8）
			IFG	0.9（0.6-1.4）
オランダ（2004）	男女 1312 名	7+と≦2 杯	糖尿病[注2)]	0.69（0.31-1.51）
縦断研究			IGT	0.37（0.16-0.84）
			IFG	1.35（0.80-2.27）

注1）1985年WHO診断基準
注2）1998年WHO診断基準
IGT: impaired glucose tolerance（耐糖能障害）
IFG: impaired fasting glycemia（空腹時血糖異常）

後高血糖を抑制することで耐糖能障害（IGT）に予防的であると考えられる。その結果として、糖尿病にも予防的であると思われる。日本の研究は男性自衛官を対象にした横断研究である。

おわりに

コーヒー飲用者では肝機能血液検査値が非飲用者に比べて良好であること、肝硬変に予防的であることが、さらに肝臓がんにも予防的であることがわかってきた。肝臓のさまざまな病気にコーヒーが予防的であることから、コーヒーの肝臓保護作用はほぼ間違いないと考えられる。γ-GTPや肝硬変の一部の研究ではコーヒーがアルコールによる肝障害に特に予防的であると指摘されているが、肝炎ウイルスに起因する肝硬変や肝がんに対しても予防的であることから、コーヒーは肝臓に全般的に良いと思われる。

さまざまな集団において、コーヒーが2型糖尿病および耐糖能障害（IGT）に予防的であることが観察されていることは重要なことである。ほとんどすべての研究で、2型糖尿病発症と密接に関係している肥満と運動の影響が考慮されている。予防的であるコーヒーの成分は特定されていないが、コーヒーが耐糖能障害（IGT）および2型糖尿病に予防的であることもほぼ間違いないと考えられる。

文献

1) Arnesen E, Huseby NE, Brenn T, et al. The Tromso Heart Study: Distribution of, and determinants for, gamma-glutamyltransferase in a free-living population. Scand J Lab Invest 1986; 46: 63-70.

2) Nilssen O, Forde OH, Brenn T. The Tromso Heart Study: Distribution and population determinants of gamma-glutamyltransferase. Am J Epidemiol 1990; 132: 318-326.

3) Casiglia E, Spolaore P, Ginocchio G, et al. Unexpected effects of coffee consumption on liver enzymes. Eur J Epidemiol 1993; 9: 293-297.

4) Nilssen O, Forde OH. Seven-year longitudinal population study of change in gamma-glutamyltransferase: The Tromso Heart Study. Am J Epidemiol 1994; 139: 787-792.

5) Kono S, Shinchi K, Imanishi K, et al. Coffee and gamma-glutamyltransferase: A study of self-defense officials in Japan. Am J Epidemiol 1994; 139: 723-727.

6) Sharp DS, Benowitz NL,: Re: "Alcohol, smoking, coffee, and cirrhosis" and "coffee and gamma-glutamyltransferase: a study of self-defense officials in Japan." Am J Epidemiol 1995; 141: 480-481.
7) Poikolainen K, Vartiainen E. Deteminants of -glutamymyltransferase: positive interaction with alcohol and body mass index, negative association with coffee. Am J Epidemiol 1997; 146: 1019-1024.
8) Tanaka K, Tokunaga S, Kono S, et al. 1998: coffee consumption and decreased serum gamma-glutamyltransferase and aminotransferase activities among male alcohol drinkers. Int J Epidemiol 27: 438-443.
9) Honjo S, Kono S, Coleman MP, et al. Coffee drinking and serum gamma-glutamyltransferase: an extended study of self-defense officials in Japan. Ann Epidemiol 1999; 9: 325-331.
10) Nakanishi N, Nakamura K, Nakajima K, et al. Coffee consumption and decreased serum gamma-glutamyltransferase: a study of middle-aged Japanese men. Eur J Epidemiol 2000; 16: 419-423.
11) Nakanishi N, Nakamura K, Suzuki K, et al. Lifestyle and the development of increased serum gamma-glutamyltransferase in middle-aged Japanese men. Scand J Clin Lab Invest 2000; 60: 429-438.
12) Nakanishi N, Nakamura K, Suzuki K, et al. Effects of coffee consumption against the development of liver dysfunction: a 4-year follow-up study of middle-aged Japanese male office workers. Ind Health 2000; 38: 99-102.
13) Honjo S, Kono S, Coleman MP, et al. Coffee consumption and serum aminotransferases in middle-aged Japanese men. J Clin Epidemiol 2001; 54: 823-829.
14) Ruhl CE, Everhart JE. Coffee and caffeine consumption reduce the risk of elevated serum alanine aminotransferase activity in the United States. Gastroenterology 2005; 128: 24-32.
15) Klatsky AL, Armstrong MA. Alcohol, smoking, coffee, and cirrhosis. Am J Epidemiol 1992; 136: 1248-1257.
16) Corrao GA, Lepore R, Torchio P, et al. The effect of drinking coffee and smoking cigarettes on the risk of cirrhosis associated with alcohol consumption. Eur J Epidemiol 1994; 10: 657-664.
17) Corrao G, Zambon A, Bagnardi V, et al. Coffee, caffeine, and the risk of liver cirrhosis. Ann Epidemiol 2001; 11: 458-465.
18) Gallus S, Tavani A, Negri E, et al. Does coffee protect against liver cirrhosis? Ann Epidemiol 2002; 12: 202-205.
19) Tverdal A, Skurtveit S. Coffee intake and mortality from liver cirrhosis. Ann Epidemiol 2003; 13: 419-423.
20) Gallus S, Bertuzzi M, Tavani A, et al. Does coffee protect against hepatocellular carcinoma? Br J Cancer 2002; 87: 956-959.
21) Gelatti U, Covolo L, Franceschini M, et al. Coffee consumption reduces the risk of hepatocellular carcinoma independently of its aetiology: a case-control study. J Hepatol 2005; 42: 528-534.
22) Inoue M, Yoshimi I, Sobue T, et al. Influence of coffee drinking on subsequent risk of hepatocellular carcinoma: a prospective study in Japan. J Natl Cancer Inst 2005; 97: 293-300.
23) Shimazu T, Tsubono Y, Kuriyama S, et al. Coffee consumption and the risk of primary liver cancer: Pooled analysis of two prospective studies in Japan. Int J Cancer 2005; 116: 150-154.
24) Leitzmann MF, Willett WC, Rim EB, et al. A prospective study of coffee consumption and the risk of symptomatic gallstone disease in men. JAMA 1999: 281: 2106-2112.
25) Ishizuka H, Eguchi H, Oda T, et al. Relation of coffee, green tea, and caffeine intake to gallstone disease in middle-aged Japanese men. Eur J Epidemiol 2003; 18: 401-405.
26) van Dam RM, Feskens EJ. Coffee consumption and risk of type 2 diabetes mellitus. Lancet 2002; 360: 1477-8.
27) Reunanen A, Heliovaara M, Aho K. Coffee consumption and risk of type 2 diabetes mellitus. Lancet 2003; 361: 702-703.
28) Saremi A, Tulloch-Reid M, Knowler WC. Coffee consumption and the incidence of type 2 diabetes.

Diabetes Care 2003; 26: 2211-2212.
29) Rosengren A, Dotevall A, Wilhelmsen L, et al. Coffee and incidence of diabetes in Swedish women: a prospective 18-year follow-up study. J Intern Med 2004; 255: 89-95.
30) Tuomilehto J, Hu G, Bidel S, et al. Coffee consumption and risk of type 2 diabetes mellitus among middle-aged Finnish men and women. JAMA 2004; 291: 1213-1219.
31) Salazar-Martinez E, Willett WC, Ascherio A, et al. Coffee consumption and risk for type 2 diabetes mellitus. Ann Intern Med 2004; 140: 1-8.
32) Carlsson S, Hammar N, Grill V, et al. Coffee consumption and risk of type 2 diabetes in Finnish twins. Int J Epidemiol 2004; 33: 1-2.
33) Agardh EE, Carlsson S, Ahlbom A, et al. Coffee consumption, type 2 diabetes and impaired glucose tolerance in Swedish men and women. J Intern Med 2004; 255: 645-652.
34) Yamaji T, Mizoue T, Tabata S, et al. Coffee consumption and glucose tolerance status in middle-aged Japanese men. Diabetologia 2004; 47: 2145-2151.
35) van Dam RM, Dekker JM, Nijpels G, et al. Coffee consumption and incidence of impaired fasting glucose, impaired glucose tolerance, and type 2 diabetes: the Hoorn Study. Diabetologia 2004; 47: 2152-2159.

ELSEVIER

Molecular and Cellular Endocrinology 247 (2006) 150–165

MCE
Molecular and Cellular Endocrinology

www.elsevier.com/locate/mce

Testicular zinc finger protein recruits histone deacetylase 2 and suppresses the transactivation function and intranuclear foci formation of agonist-bound androgen receptor competitively with TIF2

Rong-Hua Tao[a], Hisaya Kawate[a], Yin Wu[a], Keizo Ohnaka[a], Masamichi Ishizuka[b], Atsuto Inoue[b], Hiromi Hagiwara[b], Ryoichi Takayanagi[a,*]

[a] *Department of Geriatric Medicine, Graduate School of Medical Sciences, Kyushu University, 3-1-1 Maidashi, Higashi-ku, Fukuoka 812-8582, Japan*
[b] *Faculty of Biomedical Engineering, Toin University of Yokohama, Kurogane-cho 1614, Aoba-ku, Yokohama 225-8502, Japan*

Received 10 October 2005; received in revised form 20 December 2005; accepted 23 December 2005

Abstract

We previously reported that testicular zinc finger protein (TZF) is a corepressor for androgen receptor (AR). The present study demonstrated that a central portion (amino acids 512–663) of TZF, TZF(512–663), is responsible for both binding to AR and repressing the transactivation. TZF recruited endogenous histone deacetylase 2 (HDAC2) and formed a complex with agonist-bound AR. Imaging analyses showed that TZF and TZF(512–663) were recruited by AR and simultaneously impaired distinct AR foci formation. Quantification of the foci number using a three-dimensional imaging method revealed that the number of intranuclear AR foci was related to its transactivation activity. Moreover, increased levels of TZF dissociated a coactivator, TIF2, from the AR foci and vice versa. These results indicate that the ligand-dependent transactivation function of AR is quantitatively related to its intranuclear foci formation, and suggest that corepressors, such as TZF, act on these intranuclear events competitively with coactivators.

Keywords: Androgen receptor; GFP; HDAC; Corepressor

1. Introduction

Androgens regulate a wide range of developmental and physiological processes and play particularly central roles in the expression of the male phenotype. These biological actions of androgens are mediated through androgen receptor (AR), a member of the nuclear receptor superfamily (Mangelsdorf et al., 1995; Roy et al., 1999; Heinlein and Chang, 2002). Dysfunction of AR through mutations predominantly leads to three different pathological situations, namely androgen insensitivity syndrome (AIS), spinal bulbar muscular atrophy (SBMA, Kennedy's disease) and prostate cancer (Gottlieb et al., 1999; Brinkmann, 2001; Yeh et al., 2002; Kawano et al., 2003). Similar to other members of the nuclear receptor superfamily, AR is composed of four functional domains: the N-terminal transcription activation domain, DNA-binding domain (DBD), hinge region and C-terminal ligand-binding domain (LBD). The N-terminal domain contains the major ligand-independent transactivation function domain (AF-1) and the C-terminal domain contains another ligand-dependent transactivation function domain (AF-2). The DBD consists of two zinc finger clusters, of which the first zinc finger is involved in specific recognition of androgen-responsive elements (AREs) in target genes (Brinkmann, 2001; Heinlein and Chang, 2002). Before ligand binding, AR is located in the cytoplasm where it is sequestered by heat shock proteins, which maintain the receptor in a conformation that is able to bind its ligand. Ligand binding causes a conformational change of AR that releases it from the heat shock proteins and allows its translocation into the nucleus, where it binds to AREs and activates the transcription of its target genes (Gobinet et al., 2002; Gelmann, 2002). We previously reported that AR forms intranuclear fine foci in a ligand-dependent manner and is colocalized with coactivators (Tomura et al., 2001; Saitoh et al., 2002). Since treatment with antagonists and coexpression of a corepressor inhibited the AR foci formation, this foci formation was suggested to be a critical

* Corresponding author. Tel.: +81 92 642 6912; fax: +81 92 642 6911.
E-mail address: takayana@geriat.med.kyushu-u.ac.jp (R. Takayanagi).

0303-7207/$ – see front matter © 2006 Elsevier Ireland Ltd. All rights reserved.
doi:10.1016/j.mce.2005.12.052

step for transactivation by steroid receptors (Fejes-Tóth et al., 1998; Stenoien et al., 2000; Tomura et al., 2001; Saitoh et al., 2002; Kawate et al., 2005).

To date, many coregulators (coactivators and corepressors) that modulate nuclear receptor-mediated transactivation have been identified (Heinlein and Chang, 2002; Gobinet et al., 2002). One mechanism for the regulation by these coactivators and corepressors is chromatin modifications, such as acetylation or deacetylation of chromosomal histone proteins (Ogryzko et al., 1996; Heinzel et al., 1997; Kinyamu and Archer, 2004). Many coactivators carry histone acetylase activity and corepressor complexes often contain histone deacetylase (HDAC). Reversible acetylation of the core histones modulates chromatin structure and regulates transcription (Aranda and Pascual, 2001; Heinlein and Chang, 2002; Gobinet et al., 2002). It has recently been suggested that coregulators may be closely associated with the pathogenesis of several diseases, such as hormone-dependent cancers (breast or prostate cancer) and AIS (Adachi et al., 2000; Yanase et al., 2004).

Testicular zinc finger protein (TZF) has a Zn-finger motif in its C-terminus and is predominantly expressed in the testes (Inoue et al., 2000). We previously showed that TZF is a novel corepressor of AR (Ishizuka et al., 2005). TZF was localized in the nucleus in discrete dots, and recruited into AR foci after addition of the ligand 5α-dihydrotestosterone (DHT) (Ishizuka et al., 2005).

In the present study, the repression mechanism of AR by TZF was further investigated. We found that HDAC2 was involved in the TZF-mediated repression. The number of AR foci decreased with increasing levels of TZF but recovered in the presence of the coactivator TIF2. TZF and TIF2 were colocalized with agonist-bound AR, and increased levels of TZF dissociated TIF2 from the AR foci, and vice versa. These results suggest that TZF and coactivators compete for AR foci formation and AR-mediated transcriptional activation.

2. Materials and methods

2.1. Plasmid construction

Expression plasmids for AR (pCMV-hAR, pAR-GFP and pAR-CFP) were prepared as previously described (Adachi et al., 2000; Tomura et al., 2001; Saitoh et al., 2002). Firefly reporter plasmids for AR (pGL3-MMTV and pGL3-PSA) were constructed as previously described (Tomura et al., 2001; Kawate et al., 2005). The expression plasmid for TIF2 (pcDNA-TIF2) was also described previously (Saitoh et al., 2002). Expression plasmids for TZF, pEGFP-TZF and pEYFP-TZF, were constructed as follows. The plasmid pLP-EGFP-C1-TZF (Ishizuka et al., 2003) was digested with *Sal*I and *Xho*I, resulting in the creation of a *Sal*I–*Xho*I fragment encoding the C-terminus of TZF and a *Sal*I–*Sal*I fragment encoding the rest of TZF. The *Sal*I–*Xho*I fragment was initially inserted into the *Sal*I sites of pEGFP-C1 and pEYFP-C1 (BD Sciences Clontech, Palo Alto, CA), followed by insertion of the *Sal*I–*Sal*I fragment into the *Sal*I sites of these plasmids. Similarly, another expression plasmid for TZF, pFLAG-CMV2-TZF, was constructed using pFLAG-CMV2 (Sigma–Aldrich Co., St. Louis, MO). An expression plasmid for TZF(1–275), pEYFP-TZF(1–275), was constructed by removing an *Apa*I fragment from pEYFP-TZF. Subsequently, the removed *Apa*I fragment was inserted into the *Apa*I site of pEYFP-C1 to create an expression plasmid for TZF(275–942), pEYFP-TZF(275–942). A *Xho*I–*Sca*I fragment of pEYFP-TZF encoding TZF(1–663) was inserted into the *Xho*I and *Sma*I sites of pEYFP-C1 to produce pEYFP-TZF(1–663). A *Bam*HI-fragment encoding TZF(512–942) from pEYFP-TZF was cloned into the *Bam*HI site of pEGFP-C3 (BD Biosciences Clontech) to produce an expression plasmid for TZF(512–942), pEGFP-TZF(512–942). An expression plasmid for TZF(512–663), pEGFP-TZF(512–663), was constructed by inserting a *Bam*HI fragment of pEYFP-TZF(1–663) into the *Bam*HI site of pEGFP-C3. To construct an expression plasmid for an internal deletion mutant, the *Bam*HI-fragment encoding TZF(512–942) was first removed from pEYFP-TZF and a PCR-amplified fragment encoding TZF(663–942) was inserted into the *Bam*HI site of the residual plasmid to produce pEYFP-TZF(Δ512–663). The sequences of the PCR primers were 5′-AGGATCCAGGCTCAATTTCTGTAAAGCG-3′ and 5′-AGGATCCCTACTGGCCACAAGGACG-3′. The expression plasmid pFLAG-CMV2-TZF(512–663) was constructed by inserting a *Hind*III–*Xba*I fragment of pEGFP-TZF(512–663) into the *Hind*III and *Xba*I sites of pFLAG-CMV2.

To construct VP16-fusion proteins for modified mammalian one-hybrid assays, a *Kpn*I fragment of pEYFP-TZF was inserted into the *Kpn*I site of pACT (Promega Corp., Madison, WT) to construct pVP16-TZF encoding full-length TZF. An expression plasmid for TZF(1–275), pVP16-TZF(1–275), was constructed by inserting a *Sma*I fragment of pEYFP-TZF(1–275) into the *Bam*HI site of pACT which was filled with the Klenow fragment of *Escherichia coli* DNA polymerase I to create a blunt end. An expression plasmid for TZF(1–663), pVP16-TZF(1–663), was constructed by inserting a *Xho*I–*Sca*I fragment of pEYFP-TZF into the *Sal*I and *Eco*RV sites of pACT. An expression plasmid for TZF(512–663), pVP16-TZF(512–663), was constructed by inserting a *Bam*HI fragment of pEGFP-TZF(512–663) into the *Bam*HI site of pACT. To construct an internal deletion mutant fused with VP16, the insert of pEYFP-TZF(Δ512–663) was subcloned into pACT to create pVP16-TZF(Δ512–663). The validity of all the constructs was confirmed by DNA sequencing.

2.2. Cell culture

A monkey kidney-derived cell line, COS-7, was obtained from the Riken Cell Bank (Tokyo, Japan). A human prostatic cancer cell-line, LNCaP, and a mouse fibroblast cell line, NIH3T3, were obtained from the American Type Culture Collection (Manassas, VA). COS-7 and NIH3T3 cells were maintained in Dulbecco's Modified Eagle's medium (DMEM), while LNCaP cells were cultured in Roswell Park Memorial Institute 1640 medium (Sigma). Both media were supplemented with 10% fetal bovine serum (FBS; Sanko Junyaku Co. Ltd., Tokyo, Japan) and 100 U/ml of penicillin–streptomycin (Invitrogen Corp., Carlsbad, CA).

2.3. Functional reporter assay

Cells (1×10^5 cells/well) were seeded in 12-well plates and incubated for 24 h before transfection. The cells were transfected with 0.3 μg/well of pGL3-MMTV or pGL3-PSA as a reporter, 2 ng/well of pRL-CMV (a *Renilla* Luciferase vector; Promega Corp.) as an internal control, 0.1 μg/well of pCMV-hAR and 0.5 μg/well of an expression vector for full-length TZF or its truncated mutants, unless otherwise indicated, using 2.7 μl of Superfect transfection reagent (Qiagen GmbH, Hilden, Germany). In all cotransfection studies, the total amount of plasmid DNA was fixed by adding empty vector to the transfection mixture. After incubation for 3 h, the cells were rinsed with phosphate-buffered saline (PBS) and re-fed with the appropriate medium containing 10% charcoal-stripped FBS in the presence or absence of 10 nM DHT. After an additional incubation for 24 h (COS-7) or 48 h (LNCaP), the cells were lysed using the lysis buffer supplied with the luciferase kit (Promega) and the luciferase activities were assayed using the Dual-Luciferase Reporter Assay System (Promega) and a Lumat LB 9507 luminometer (Berthold Technologies, Bad Wildbad, Germany). An additional treatment with trichostatin A (TSA; Sigma) was carried out for 12 h before cell harvesting. One-way analysis of variance followed by Scheffé's test was used for multigroup comparisons. $P < 0.05$ was considered to be statistically significant.

2.4. Modified mammalian one-hybrid assay

NIH3T3 cells (1×10^5 cells/well) were seeded in 12-well plates at 24 h before transfection. The cells were transiently transfected with 0.3 μg of an expression vector for full-length TZF or its truncated mutants fused to VP16,

0.1 μg of pCMV-hAR, 0.3 μg of pGL3-MMTV and 2 ng of pRL-CMV. The cells were then incubated with or without 10 nM DHT for 24 h and the luciferase activities were measured as described above.

2.5. Coimmunoprecipitation and immunoblot analysis

COS-7 or LNCaP cells (1×10^6 cells/dish) were seeded in 100 mm culture dishes and transiently transfected with 7.5 μg of a plasmid expressing GFP-tagged full-length TZF or its truncated mutants and 1.5 μg of pCMV-hAR, followed by incubation with or without 10 nM DHT for 24 h. The cells were lysed in a buffer consisting of 20 mM HEPES–NaOH, pH 7.9, 20% glycerol, 100 mM KCl, 0.2 mM EDTA, 0.5% NP-40 and a protease inhibitor cocktail (Roche Diagnostics, Tokyo, Japan) at 4 °C for 30 min, followed by a brief sonication. The lysates were collected by centrifugation. The protein concentrations were measured using a BCA protein assay kit (Pierce, Rockford, IL) and each protein concentration was adjusted to 1 mg/ml. For immunoprecipitation analyses, antibodies against green fluorescent protein (GFP) and AR (C-19) (Santa Cruz Biotechnology, Santa Cruz, CA) were preincubated with Protein A magnetic beads (New England Biolabs Inc., Beverly, MA) at 4 °C for 2 h. Each lysate (200 μg) was then incubated with 10 μg of the anti-GFP or -AR antibody-conjugated beads in WB buffer (20 mM HEPES–NaOH, pH 7.9, 20% glycerol, 100 mM KCl, 0.2 mM EDTA, 0.5% NP-40 and 0.5% skim milk) at 4 °C overnight. After the beads had been washed four times with 180 μl of WB buffer and four times with 180 μl of WH buffer (20 mM HEPES–NaOH, pH 7.9, 20% glycerol, 100 mM KCl, 0.2 mM EDTA and 0.5% NP-40), the bound proteins were eluted in 60 μl of 2× sodium dodecyl sulfate-polyacrylamide gel electrophoresis (SDS-PAGE) sample buffer (4% SDS, 200 mM dithiothreitol, 120 mM Tris–HCl, pH 6.8 and 0.02% bromophenol blue) and subjected to 10% SDS-PAGE at 20 mA for 4 h. Immunoblotting analyses were then performed as previously described (Kawate et al., 2005). Briefly, proteins were transferred onto a nitrocellulose membrane (Hybond ECL; Amersham Biosciences Corp., Piscataway, NJ) using a Hoefer miniVe unit (Amersham) at 250 V for 1 h at 25 °C. The membrane was blocked in 1× Block-Ace (Dainippon Pharmaceutical Co., Osaka, Japan) and reacted with an appropriate primary antibody in 0.1× Block-Ace for 1 h at 25 °C. Following a brief wash with TBS–Tween 20 (10 mM Tris–HCl, pH 8.0, 0.9% NaCl and 0.05% Tween 20), the membrane was incubated with a horseradish peroxidase-conjugated secondary antibody (Amersham) in 0.1× Block-Ace for 45 min at 25 °C. After washing with TBS–Tween 20, the membrane was reacted with ECL western blotting detection reagents (Amersham) and the bands were detected using a Versa-Doc Model 5000 Imaging System (Bio-Rad Laboratories, Hercules, CA).

2.6. HDAC activity assay

Polyclonal anti-TZF antibodies were obtained by subcutaneously injecting rabbits with 50 μg of the C-terminal 41 amino acids of TZF once per week for 4 weeks. COS-7 cells (1×10^6 cells/dish) were seeded in 100 mm culture dishes and transfected with 7 μg of pEGFP-TZF or pEGFP. After incubation for 24 h, cell lysates were prepared and incubated with the anti-TZF antibodies in the presence of Protein A magnetic beads. Immunoprecipitates were subjected to HDAC activity assays using an HDAC fluorescent activity assay kit (AK-500; Biomol Research Laboratories, Plymouth Meeting, PA) according to the manufacturer's recommended protocol. The beads were resuspended in 100 μl of 250 μM Fluor de Lys substrate in the presence or absence of 5 μM TSA and incubated with rocking at 25 °C for 90 min. Next, 25 μl of each reaction mixture was added to 25 μl of assay buffer (25 mM Tris–HCl, pH 8.0, 137 mM NaCl, 2.7 mM KCl and 1 mM $MgCl_2$) and 50 μl of 1× Fluor de Lys Developer with 2 μM TSA, and incubated for 15 min at 25 °C to stop the HDAC reaction. The HDAC activities were measured by excitation with 360 nm light and emission of 460 nm light using an ARVO SX 1420 multilabel counter (Wallac, Turku, Finland).

2.7. Confocal laser scanning microscopy

For living cell microscopy, COS-7 cells (2×10^5 cells/dish) were cultured in 35 mm glass-base dishes (Asahi Techno Glass Corp., Tokyo, Japan) and transfected with pAR-GFP or pAR-CFP and GFP (YFP)-tagged full-length TZF or its truncated mutants using Superfect reagents (Qiagen). After incubation for 3 h, the cells were washed with PBS, maintained in DMEM supplemented with 10% charcoal-treated FBS for 16–20 h and then incubated in the presence or absence of 10 nM DHT. The cells were observed with an Axiovert 200M inverted microscope equipped with an LSM 510 META scan head (Carl Zeiss Co. Ltd., Jena, Germany) using a 100× 1.4 numerical aperture oil immersion objective as described previously (Kawate et al., 2005). Images were collected at a 12-bit depth resolution of intensities over 1024 × 1024 pixels. For excitation of CFP, GFP and YFP, 458 and 488 nm argon lasers were employed and the emission signals were separated using the emission fingerprinting technique established by Carl Zeiss. Separation of the individual emission signals was based on recordings of the spectral signature of each emission signal and a digital unmixing procedure using these reference spectra. A three-dimensional imaging study was performed as previously described (Saitoh et al., 2002). Briefly, a series of 30–50 two-dimensional images were collected for each nucleus using a confocal laser microscope, and reconstructed using the three-dimensional analysis software of the TRI Graphics Program (Ratoc System Engineering, Tokyo, Japan). Both the spatial distribution and calculation of the fluorescent proteins as distinct volumes were made possible by removing scattering background fluorescence and lens spherical aberrations and then separating each particle. The analytical conditions were kept constant throughout all the experiments. The numbers of subnuclear foci were representative of at least 15 cells.

2.8. Immunostaining

COS-7 cells (2×10^4 cells/well) were seeded in Lab-Tek II Chamber Slides (Nalge Nunc International, Naperville, IL) and transfected with pEGFP-TZF using 1 μl/well of the Superfect reagent. After incubation for 24 h, the cells were washed with PBS and fixed with 50% methanol/50% acetone for 10 min at −20 °C. After blocking in 1× Block-Ace for 10 min at 25 °C, the cells were incubated with an anti-HDAC2 goat polyclonal IgG antibody (Santa Cruz; 1:200 dilution in 0.1× Block-Ace) for 1 h at 25 °C. Following a brief wash with TBS–Tween 20, the cells were incubated with Alexa Fluor 546-conjugated donkey anti-goat IgG (H + L) (Molecular Probes Inc., Eugene, OR; 1:400 dilution in 0.1× Block-Ace) for 1 h at 25 °C. After washing with TBS–Tween 20, the cells were mounted in Vectashield (Vector Laboratories, Burlingame, CA) and observed under a confocal laser scanning microscope using 488 nm (argon) and 543 nm (helium-neon) laser lines for excitation of GFP and Alexa Fluor 546, respectively.

2.9. Fluorescence recovery after photobleaching (FRAP) analysis

COS-7 cells (2×10^5 cells/dish) were seeded in 35 mm glass-base dishes and transfected with various plasmids as described above. After addition of the ligand, FRAP analysis was performed by confocal laser scanning microscopy essentially as previously described (Stenoien et al., 2001). After collection of the initial image, a selected area of a fixed size (region of interest, ROI) in the nucleus was photobleached using the maximum power of the 488 nm argon laser for 70 iterations. After the bleaching, images were taken every 0.5 s at a resolution of 256 × 256 pixels to follow the recovery of the fluorescence intensity in the ROI. The fluorescence intensities of the ROI were calculated using the LSM software and the half-recovery time ($t_{1/2}$) was determined using the Microsoft Excel software.

3. Results

3.1. A central domain of TZF is required for repression of AR-mediated transactivation

Using different promoters and cells, we confirmed that AR-mediated transactivation was repressed by TZF in a dose-dependent manner (Fig. 1A and B). Endogenous AR-mediated transactivation was also inhibited by expression of TZF (Fig. 1B). To determine the repression domain in the TZF protein, various TZF deletion mutants were constructed (Fig. 2A) and subjected to functional promoter assays in COS-7

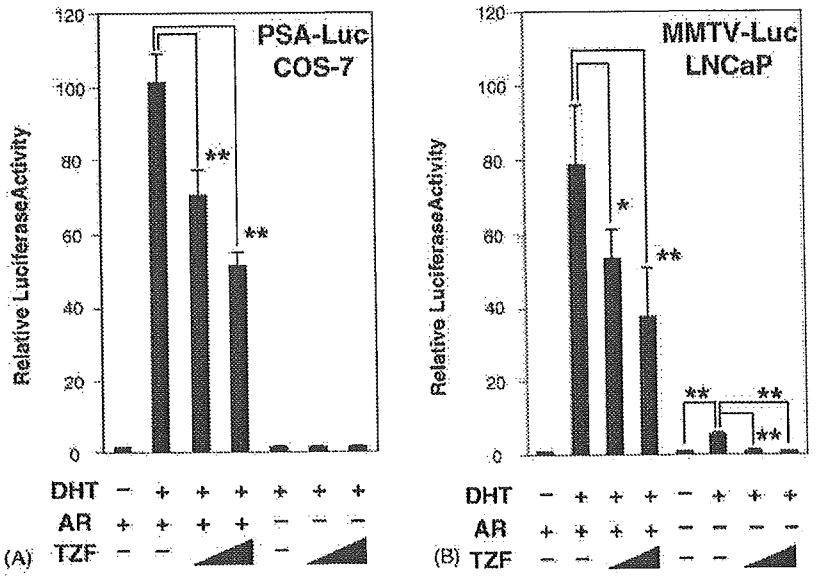

Fig. 1. Repression of AR-mediated transactivation by TZF. COS-7 (A) and LNCaP (B) cells were cotransfected with pGL3-PSA (A) or pGL3-MMTV (B) as a reporter and pRL-CMV as an internal control, with or without pCMV-hAR and pFLAG-CMV2-TZF. The amounts of the transfected plasmids were described in Section 2, except for the use of 0.5 or 1.0 μg of pFLAG-CMV2-TZF. The cells were incubated in the absence or presence of 10 nM DHT for 24 h and the luciferase activities were measured. The right-hand three bars in (A) and four bars in (B) show the results of control cells without transfection of the AR expression vector. Bars show the fold change in the luciferase activity relative to the value induced by AR without DHT. The data represent the means ± S.D. of three independent experiments. $^{*}P<0.05$; $^{**}P<0.01$.

cells (Fig. 2B and C). The TZF(1–275) mutant, consisting of the N-terminal region of TZF, was unable to repress AR-mediated transactivation, whereas TZF(275–942) lacking the N-terminal region showed the same level of repression as full-length TZF (Fig. 2B). These results indicate that the N-terminus is not involved in the repression function of TZF. Surprisingly, two other truncated mutants of TZF, namely TZF(1–663) and TZF(512–942), showed much stronger repression of AR-mediated transactivation than wild-type TZF (Fig. 2B). Since the common amino acid sequence between these two strong mutants consisted of residues 512–663, we examined the effects of TZF(512–663) comprising these amino acids and TZF(Δ512–663) lacking these amino acid residues on the transactivation activity for AR (Fig. 2A). As shown in Fig. 2C, TZF(512–663) repressed AR-mediated transcriptional activation as strongly as TZF(1–663) and TZF(512–942), whereas TZF(Δ512–663) had no effect. These results indicate that amino acid residues 512–663 are essential for the repressive effect of TZF on AR-mediated transactivation.

3.2. Interaction between the central domain (512–663) of TZF and AR

To examine whether the TZF(512–663) domain could interact with AR, modified mammalian one-hybrid assays were performed. In this system, expression plasmids for AR and VP16-fused proteins of interest were cotransfected with an MMTV promoter-luciferase reporter plasmid into NIH3T3 cells. If the protein of interest was able to interact with AR, transactivation would be enhanced compared to the basic activity of AR without the VP16-fused protein. Although the N-terminus of TZF, TZF(1–275), was unable to enhance the transactivation, full-length TZF, TZF(1–663) and TZF(512–663) enhanced the reporter activity, indicating that these three proteins were able to interact with AR (Fig. 3B). The internal deletion mutant TZF(Δ512–663) was unable to enhance the luciferase activity (Fig. 3B).

We previously demonstrated that full-length TZF coimmunoprecipitated with AR (AR-AF-1 domain) (Ishizuka et al., 2005). Therefore, coimmunoprecipitation analyses were performed to investigate the interaction between AR and the truncated TZF mutants. GFP-tagged full-length TZF or its truncated mutants and AR were coexpressed in COS-7 cells, and cell extracts were immunoprecipitated with an anti-AR or anti-GFP antibody. As shown in Fig. 4, AR was coimmunoprecipitated with full-length TZF and TZF(512–663), but not with TZF(Δ512–663). These results further confirm that TZF(512–663) is able to interact with AR.

3.3. HDAC activity is involved in the TZF-repression complex

HDAC activity is often identified in corepressor complexes associated with steroid hormone receptors. To investigate whether HDAC activity is related to the TZF-induced repression of AR transactivation, COS-7 cells were treated with TSA, a specific inhibitor of HDAC, and subjected to functional promoter assays. As shown in Fig. 5A, ligand-dependent AR transactivation was enhanced after TSA treatment. Although coexpression of TZF repressed AR-mediated transactivation, TSA completely

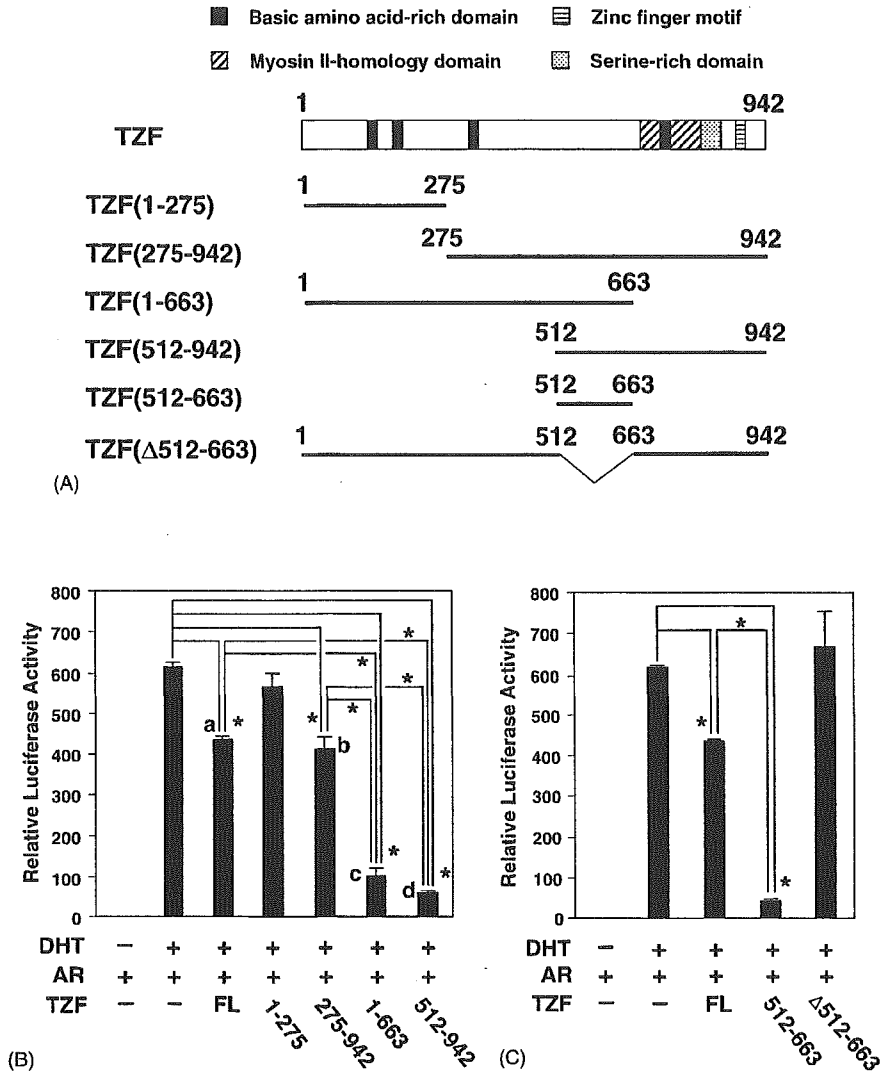

Fig. 2. Identification of the repression domain in TZF for AR-mediated transactivation. (A) Schematic representation of full-length TZF and its various truncated mutants. Several conserved domains including a zinc finger motif are indicated. (B) Effects of full-length TZF and its truncated mutants on AR-mediated transactivation. (C) The TZF(512–663) domain is required for the repression of AR-mediated transactivation by TZF. COS-7 cells were transiently transfected with pGL3-MMTV, pRL-CMV, pCMV-hAR and an expression plasmid for full-length TZF (FL) or its truncated mutants as described in Section 2. The transfected cells were incubated with or without 10 nM DHT for 24 h and the luciferase activities were measured. Bars show the fold change in the luciferase activity relative to the value induced by AR without DHT. The data represent the means ± S.D. of three independent experiments. $^{*}P<0.01$. a and b > c and d ($P<0.01$).

abolished this effect (Fig. 5A). We further tested whether the strong repressive effect of TZF(512–663) was influenced by TSA. As shown in Fig. 5B, TSA was able to reverse the repression by TZF(512–663) in a dose-dependent manner. To further confirm HDAC involvement in the TZF-repression complex, TZF was immunoprecipitated by an anti-TZF antibody and the immunoprecipitate was subjected to an HDAC activity assay. The immunoprecipitate from the TZF-expressing cells showed remarkably higher HDAC activity than that from cells without expression of TZF. Abolishment of the HDAC activity by TSA confirmed that the TZF-immunocomplex contained HDAC activity (Fig. 5C). These results indicate that HDAC activity is involved in the TZF-induced repression of AR-mediated transactivation.

To investigate which HDAC protein is involved in the TZF-induced repression of AR, immunoblot analyses with several anti-HDAC antibodies were performed on immunoprecipitates pulled down by an anti-GFP antibody from GFP-TZF expressing COS-7 cells. The results revealed that HDAC2 was coimmunoprecipitated with TZF (Fig. 6A), whereas HDAC1 and HDAC3 were not (data not shown). To examine the intracellular localization of HDAC2, GFP-TZF-expressing COS-7 cells were immunostained with an anti-HDAC2 antibody. Endogenous HDAC2 was located in the nucleus where it formed discrete dots that were colocalized with TZF (Fig. 6B). These data indicate that TZF probably interacts with HDAC2 in the cells. We further found that TZF was able to interact with AR and HDAC2. To investigate whether these three proteins were involved in the

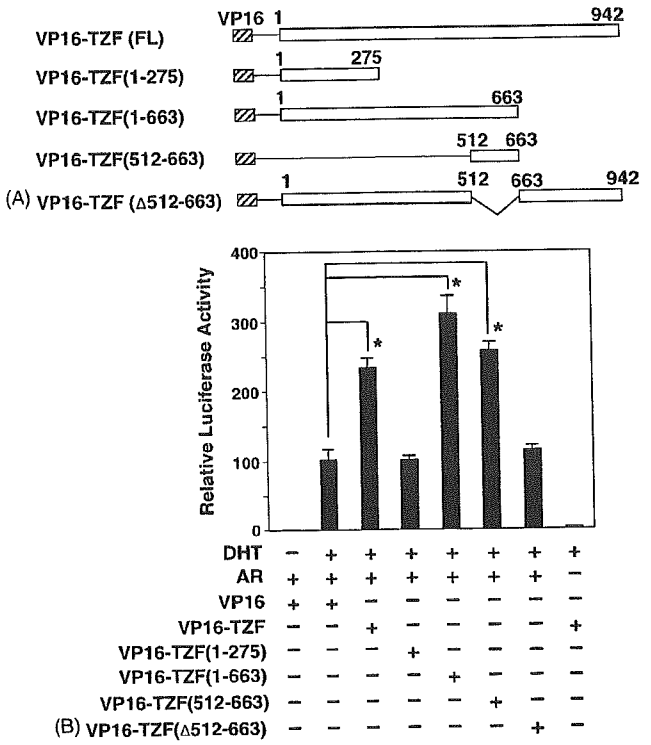

Fig. 3. Identification of the interaction domain of TZF with AR by a modified mammalian one-hybrid assay. (A) Schematic representation of VP16-fused full-length TZF (FL) and its truncated mutants. (B) A central domain (amino acids 512–663) of TZF can interact with AR. NIH3T3 cells were cotransfected with pCMV-hAR, pGL3-MMTV, pRL-CMV and an expression plasmid for VP16-fused TZF or its truncated mutants as indicated. The cells were incubated with or without 10 nM DHT for 24 h and the luciferase activities were measured. Bars show the fold change in the luciferase activity relative to the value induced by VP16 and AR without DHT. The data represent the means ± S.D. of three independent experiments. $^{*}P < 0.01$.

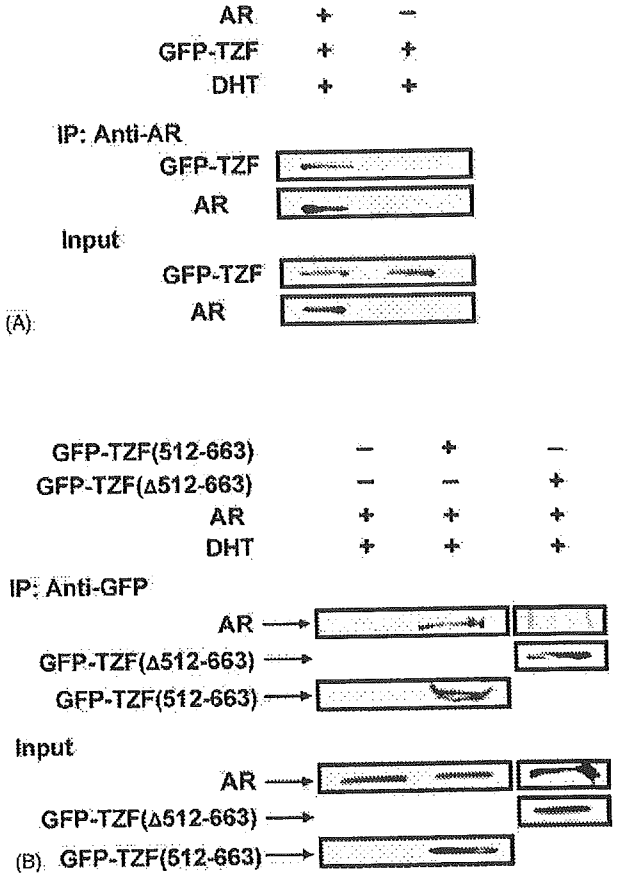

Fig. 4. Coimmunoprecipitation analyses of TZF and its truncated mutants with AR. (A) Coimmunoprecipitation of full-length TZF with AR. COS-7 cells were transfected with pEGFP-TZF and pCMV-hAR or an empty vector and incubated with 10 nM DHT for 24 h. Whole cell lysates were immunoprecipitated using an anti-AR antibody. (B) Coimmunoprecipitation of truncated TZF mutants with AR. COS-7 cells were cotransfected with pCMV-hAR and pEGFP-TZF(512–663), pEGFP-TZF(Δ512–663) or an empty vector, and treated with 10 nM DHT for 24 h. Whole cell lysates were immunoprecipitated using an anti-GFP antibody. The precipitates were subjected to immunoblot analyses using an anti-AR antibody for detection of AR and an anti-GFP antibody for detection of TZF and its mutants tagged with GFP. The expression levels of AR, TZF and the truncated TZF proteins were confirmed by immunoblot analyses of the whole cell lysates.

same protein complex, coimmunoprecipitation analyses were performed using LNCaP cells expressing endogenous AR and HDAC2. After transfection of pEGFP-TZF or an empty vector, LNCaP cells were incubated with DHT and the whole cell extract was prepared for immunoprecipitation with an anti-GFP antibody. Immunoblot analysis revealed that endogenous AR and HDAC2 were coimmunoprecipitated with GFP-TZF (Fig. 6C). These results indicate that AR, TZF and HDAC2 form a ternary complex during the repression of AR-mediated transactivation.

3.4. Ligand-dependent intranuclear colocalization of TZF or its truncated mutants with AR

As reported in our previous studies using GFP-fused proteins and confocal laser microscopy (Tomura et al., 2001; Saitoh et al., 2002), AR was located in the cytoplasm in the absence of the ligand, and translocated into the nucleus to form uniform fine foci after ligand addition in COS-7 cells (Fig. 7Aa and Ab). On the other hand, TZF was localized in the nucleus where it formed discrete dots that were larger and less numerous than the ligand-induced AR foci (Fig. 7Ac). Interestingly, upon coexpression of non-fluorescent AR, the TZF dot pattern was completely changed after DHT addition and became similar to the AR foci pattern (Fig. 7Ad and Ae) as previously reported (Ishizuka et al., 2005). Using different fluorescent proteins (GFP and YFP), colocalization of these two proteins was confirmed (Fig. 7B). Thus, TZF was considered to be recruited into AR foci in a ligand-dependent manner. To examine the colocalization of TZF mutants with AR, AR and TZF mutants fused to different fluorescent proteins were coexpressed and observed under a confocal microscope. TZF(1–275) lacking the repressive effect on AR-mediated transactivation was diffusely distributed in the nucleus in the absence of the ligand. After addition of DHT, AR was translocated into the nucleus to form fine foci but TZF(1–275) remained diffuse in the nucleus and did not colocalize with AR (Fig. 7C). TZF(1–663), which repressed AR-mediated transactivation more strongly

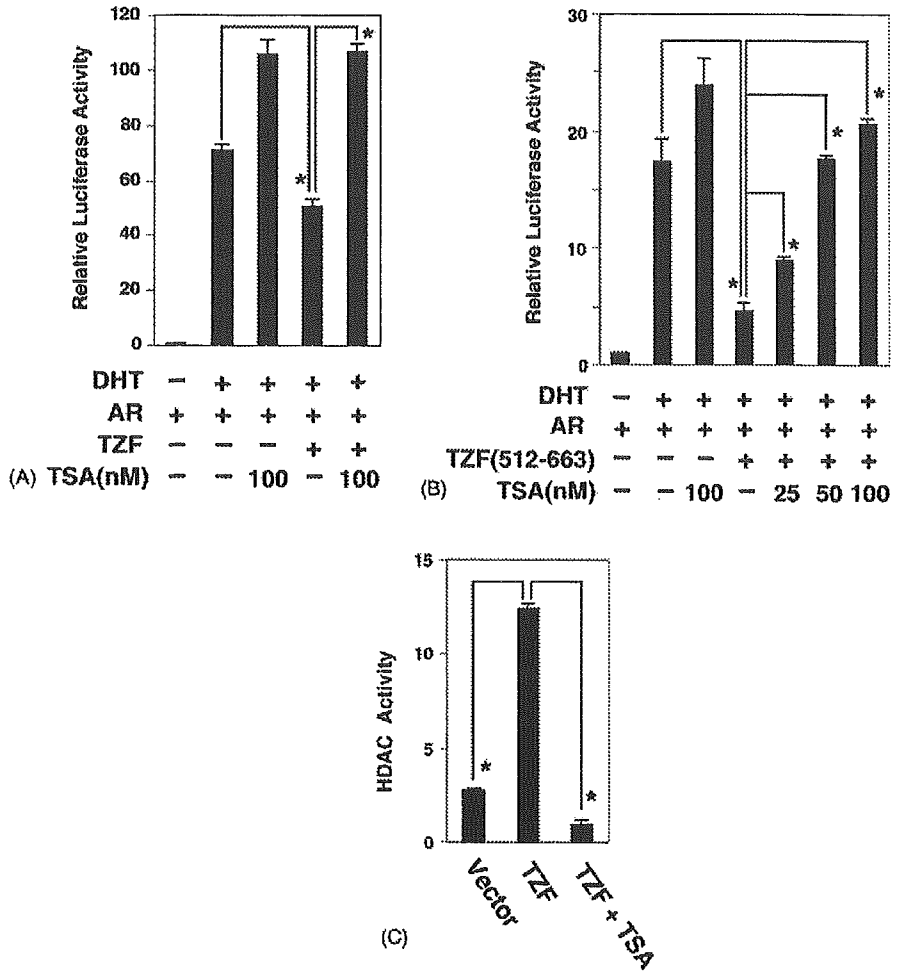

Fig. 5. HDAC activity is involved in TZF-induced repression of AR-mediated transactivation. (A) Repression of AR-mediated transactivation by TZF is recovered by TSA. (B) TZF(512–663)-induced repression of AR-mediated transactivation is recovered by TSA in a dose-dependent manner. COS-7 cells were transiently transfected with pGL3-PSA, pRL-CMV and pCMV-hAR, with or without pFLAG-CMV2-TZF (A) or pFLAG-CMV2-TZF(512–663) (B) as described in Section 2. The cells were incubated in the absence or presence of 10 nM DHT for 12 h and then left untreated or treated with TSA as indicated, followed by incubation for an additional 12 h. Next, whole cell extracts were prepared and subjected to luciferase assays. Bars show the fold change in the luciferase activity relative to the value induced by AR without DHT. The data represent the means ± S.D. of three independent experiments. $^{*}P < 0.01$. (C) TZF-immunocomplexes contain HDAC activity. COS-7 cells were transiently transfected with pEGFP or pEGFP-TZF. After incubation for 24 h, whole cell lysates were prepared and immunoprecipitated with an anti-TZF antibody. The precipitates were subjected to HDAC activity assays as described in Section 2. The data represent the means ± S.D. of three independent experiments. $^{*}P < 0.01$.

than wild-type TZF, showed a ligand-induced change in the pattern of its intranuclear dots, similar to the case for wild-type TZF. The nuclear dots of TZF(1–663) became smaller and more numerous and were colocalized with AR (Fig. 7D). TZF(512–663) also strongly repressed AR-mediated transactivation, but this mutant was diffusely distributed in both the nucleus and the cytoplasm and did not form intranuclear dots in the absence of DHT (Fig. 7E, upper panels). In the presence of the ligand, fluorescent signals for TZF(512–663) were only observed in the nucleus where they were colocalized with AR (Fig. 7E, lower panels). These colocalization results are consistent with the above-described results for the modified mammalian one-hybrid assays and coimmunoprecipitation experiments.

3.5. Correlation of the intranuclear foci number of AR with its transactivation activity

Although ligand treatment caused colocalization of TZF(512–663) with AR, the distinct intranuclear foci formation of AR seemed to be inhibited by this mutant (Fig. 7Ab and Ee), which showed strong repression of AR-mediated transactivation (Fig. 2C). These results suggested that the transactivation function of AR may be related to the number of its distinct intranuclear foci. To prove this hypothesis, we first quantified the number of intranuclear AR foci in COS-7 cells using three-dimensional images reconstructed from tomographic images collected by a confocal microscope. This method is able to detect a distinct volume by removing

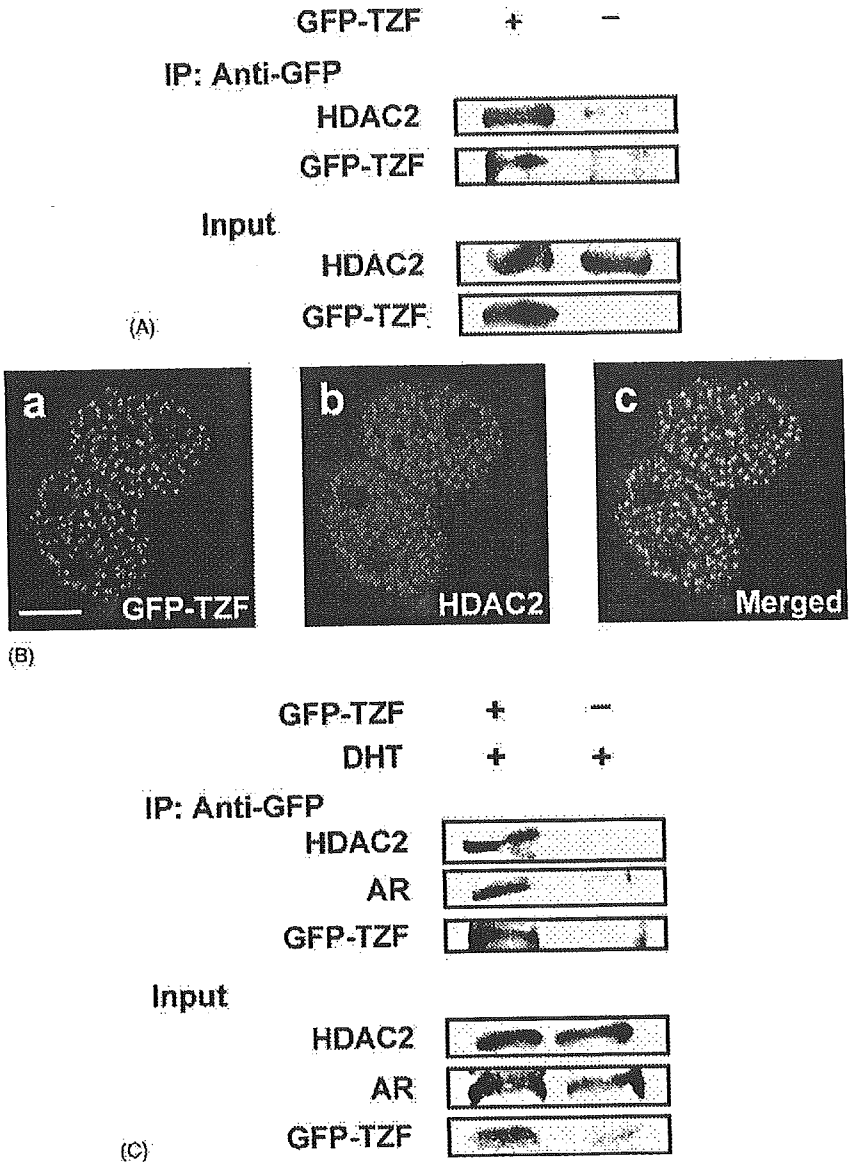

Fig. 6. HDAC2 is involved in the TZF repression complex. (A) Endogenous HDAC2 is coimmunoprecipitated with TZF. COS-7 cells were transiently transfected with pEGFP-TZF or an empty vector and incubated for 24 h. Whole cell lysates were immunoprecipitated with an anti-GFP antibody. The precipitates were subjected to immunoblot analyses with an anti-HDAC2 antibody for detection of endogenous HDAC2 and an anti-TZF antibody for detection of GFP-TZF. To confirm the expression levels of endogenous HDAC2 and transfected GFP-TZF, the whole cell lysates were directly subjected to the immunoblot analyses. (B) Colocalization of TZF with endogenous HDAC2. COS-7 cells were transiently transfected with pEGFP-TZF and incubated for 24 h. The cells were fixed and immunostained with an anti-HDAC2 antibody, followed by incubation with an Alexa Fluor 546-labeled secondary antibody. Signals for GFP-TZF (green; a) and HDAC2 (red; b) were observed by laser confocal microscopy, and the two signals were merged (c). Bar = 5 μm. (C) Endogenous AR and HDAC2 are both involved in TZF-immunocomplexes in LNCaP cells. LNCaP cells were transiently transfected with pEGFP-TZF or an empty vector and incubated in the presence of 10 nM DHT for 48 h. Whole cell lysates were immunoprecipitated with an anti-GFP antibody. The precipitates were subjected to immunoblot analyses with an anti-HDAC2 antibody for detection of HDAC2, an anti-AR antibody for detection of AR and an anti-GFP antibody for detection of GFP-TZF. To confirm the expression levels of endogenous HDAC2, AR and GFP-TZF, the whole cell lysates were also subjected to the immunoblot analyses (for interpretation of the references to colour in this figure legend, the reader is referred to the web version of the article).

background scattering fluorescence and relatively diffusely distributed fluorescence, thereby clearly showing a difference in the intranuclear spatial distribution of the foci. The number of ligand-induced intranuclear foci of AR was 317 ± 58 ($n = 15$) (Fig. 8Aa) and this was not influenced by coexpression of an empty vector, pFLAG-CMV2 or pcDNA3 (315 ± 42, $n = 18$) (Fig. 8Ab). When AR and TZF(512–663) were coexpressed at a ratio of 1:1.5, the number of AR foci was decreased to 189 ± 53 ($n = 15$) (Fig. 8Ac). Furthermore, increased TZF(512–663) at a ratio of 1:10 almost completely inhibited the AR foci formation (22 ± 16, $n = 18$) (Fig. 8Ad). Next, we tested the effect of a coactivator protein, TIF2, on the number of intranuclear AR foci. Initially, AR, TZF(512–663) and TIF2 were coexpressed at a ratio of 1:10:3. As shown in Fig. 8Ae, TIF2 expres-

sion partially recovered the number of intranuclear AR foci (101 ± 18, $n = 18$). Coexpression of an equal amount of TIF2 to TZF(512–663) at a ratio of 1:10:10 completely recovered the number of intranuclear AR foci to the basal level without the TZF mutant (318 ± 44, $n = 18$) (Fig. 8Af). The corepressor TZF(512–663) decreased the number of intranuclear AR foci, and the coactivator TIF2 was able to reverse this inhibition of AR foci formation. To compare the number of intranuclear AR foci with the transcriptional activity, functional promoter assays were performed using the same transfection conditions used for the experiments in Fig. 8A. TZF(512–663) repressed ligand-dependent AR-mediated transactivation in a dose-dependent manner (Fig. 8B). When AR and TZF(512–663) were coexpressed with TIF2 at a ratio of 1:10:3, AR-mediated

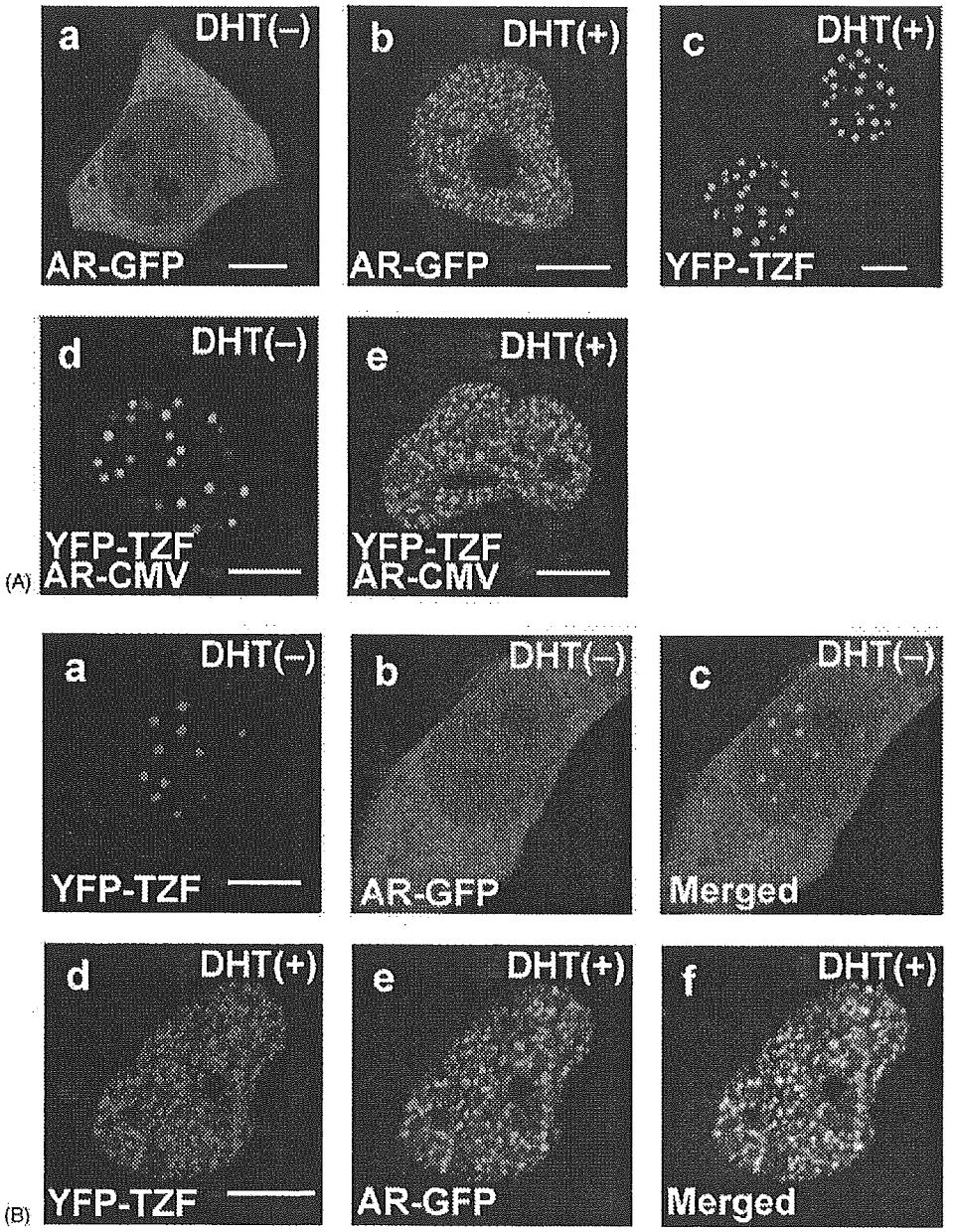

Fig. 7. Subcellular localizations of AR, full-length TZF and truncated TZF mutants. (A) Subcellular localizations of AR and TZF. COS-7 cells were transfected with pAR-GFP alone (a and b), pEYFP-TZF alone (c) or both pEYFP-TZF and pCMV-hAR (d and e) and incubated for 24 h. After incubation with or without 10 nM DHT for 1 h, the cells were observed under a laser confocal microscope. (B–E) Analyses of AR colocalization with TZF or its truncated mutants. COS-7 cells were cotransfected with pAR-GFP/CFP and pEYFP-TZF (B), pEYFP-TZF(1–275) (C), pEYFP-TZF(1–663) (D) or pEGFP-TZF(512–663) (E). The amounts of the transfected plasmids were the same as those in the functional promoter assay described in Section 2. The cells were incubated for 24 h and then further incubated in the absence (upper panels, a–c) or presence (lower panels, d–f) of 10 nM DHT for 1 h before observation by laser confocal microscopy. a and d, signals from TZF or its mutants (red); b and e, signals from AR (green); c and f, merged signals. Bars = 5 μm (for interpretation of the references to colour in this figure legend, the reader is referred to the web version of the article).

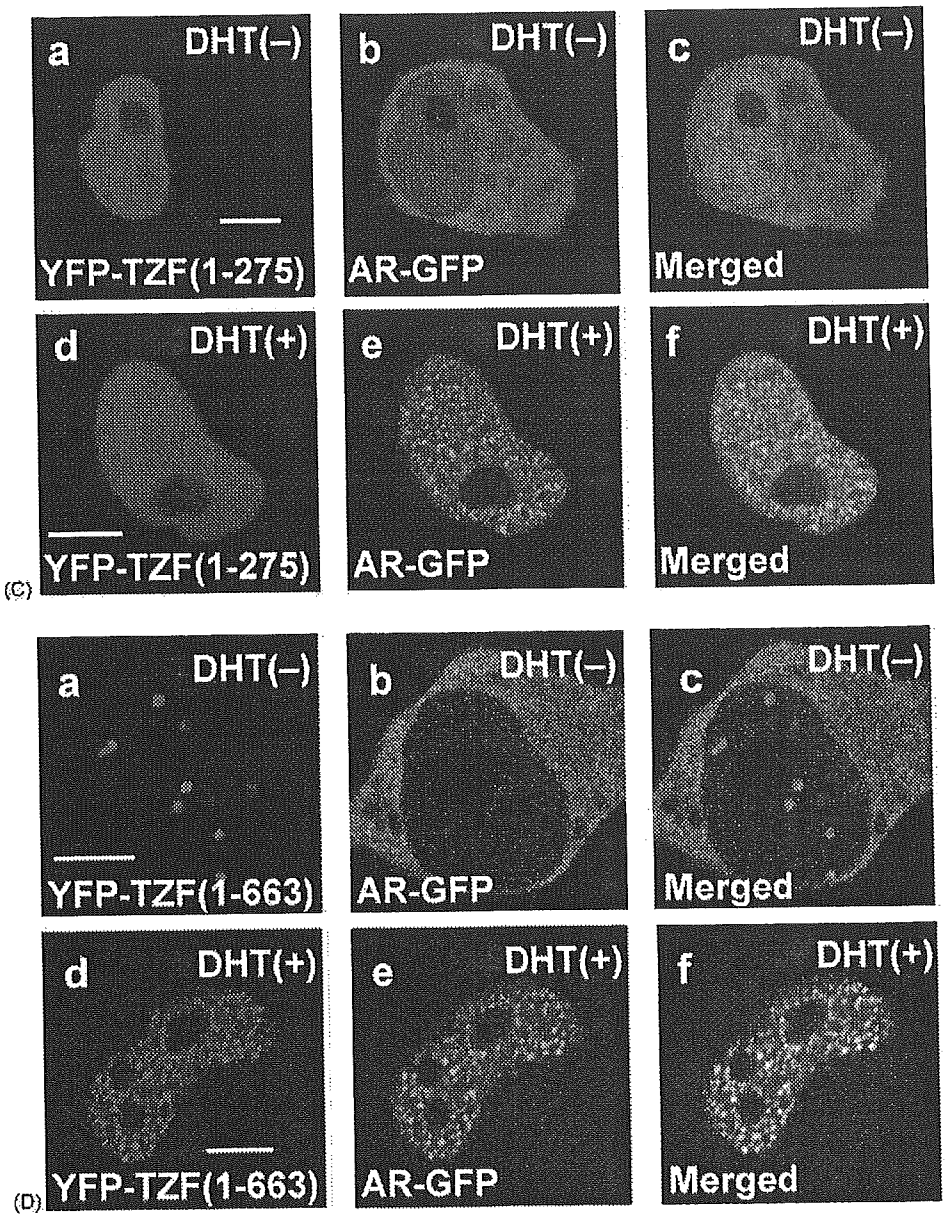

Fig. 7. (*Continued*).

transactivation was partially recovered. Moreover, when TIF2 was coexpressed at an equal level to TZF(512–663) at a ratio of 1:10:10, AR-mediated transactivation was recovered to almost the same level as that for DHT-bound AR alone (Fig. 8B). These data provide powerful evidence for our previous speculation that AR foci formation is closely linked to its transactivation function (Tomura et al., 2001; Saitoh et al., 2002).

3.6. *TIF2 is released from AR foci by coexpression of TZF*

To further analyze the competition between TIF2 and TZF for AR foci formation, the effect of TZF on the intranuclear localization of TIF2 was evaluated using COS-7 cells expressing YFP-TIF2 and AR-GFP with or without cotransfection of pFLAG-CMV2-TZF. In the absence of the ligand, TIF2 formed discrete dots in the nucleus and AR was located in the cytoplasm (Fig. 9a–c). After addition of the ligand, the discrete dots of TIF2 disappeared and it was recruited into the intranuclear AR fine foci (Fig. 9d–f). The almost complete colocalization of AR and TIF2 is characterized by the yellow color of the merged image in Fig. 9f. However, coexpression of TZF released TIF2 from the AR foci, even in the presence of DHT, and the discrete TIF2 dots reappeared (Fig. 9g–i). The green signals of AR and red signals of TIF2 were clearly separated (Fig. 9i). Conversely, the colocalization of TZF with AR (Fig. 9j–l) was impaired by coexpression of TIF2 (Fig. 9m–o) and the original TZF dots reappeared (Fig. 9n). The green signals of AR and red signals of TZF were clearly separated (Fig. 9o). These results suggest that TIF2 and TZF compete for interaction with AR in the cells.

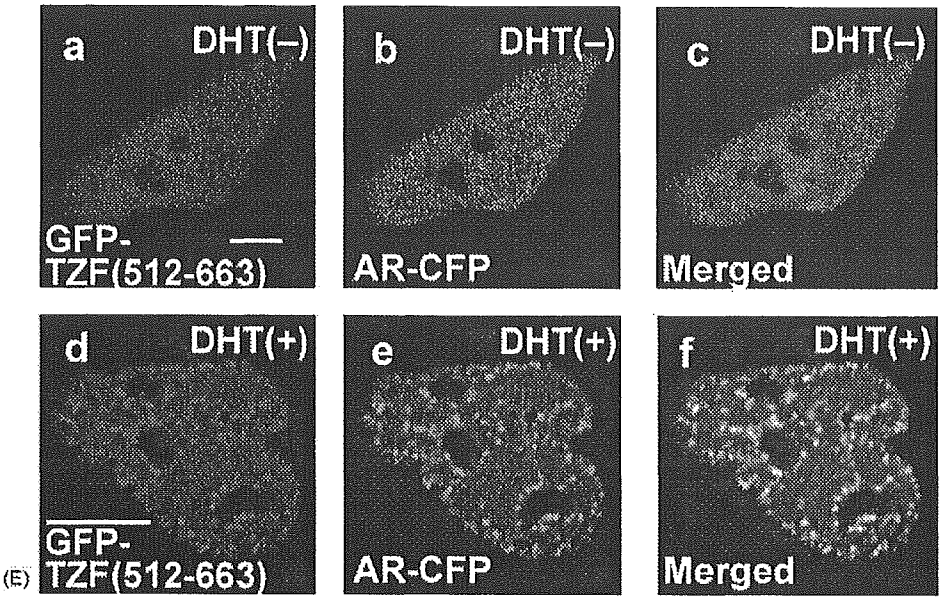

(E)

Fig. 7. (*Continued*).

3.7. Effects of TZF and TZF(512–663) on the intranuclear dynamics of AR

Previous FRAP analyses revealed that steroid hormone receptors show decreased intranuclear mobility after ligand treatment due to their association with the nuclear matrix, which is essential for ligand-induced transcriptional activation (Stenoien et al., 2001; Schaaf and Cidlowski, 2003). To examine the effects of TZF and TZF(512–663) on the intranuclear mobility of AR, FRAP experiments were performed using a confocal microscope in COS-7 cells. After treatment with DHT for 1 h, a ROI was photobleached using the maximal power of a 488 nm argon laser. After the photobleaching, images were taken every 0.5 s and the normalized fluorescence intensities of the ROI were calculated and plotted against time. In the presence of the ligand, AR-GFP-expressing cells showed fluorescence recovery and the half-recovery time was 7.5 ± 0.9 s ($n = 20$) (Fig. 10, upper panel). In this experiment, the bleached ROI could still be distinguished from unbleached regions even at 30 s after the photobleaching (Fig. 10, upper panel). Upon coexpression of full-length TZF, the bleached ROI became unclear at 30 s after the photobleaching and the half-recovery time (5.5 ± 0.9 s, $n = 15$) was shorter than that for AR alone (Fig. 10, middle panel). Furthermore, coexpression of TZF(512–663) showed much faster recovery ($t_{1/2} = 3.2 \pm 0.5$ s, $n = 15$) (Fig. 10, lower panel). These results suggest that the intranuclear mobility of AR is increased by coexpression of TZF or TZF mutants that may weaken the interaction of AR with the nuclear matrix.

4. Discussion

The mechanism of TZF-induced repression of AR-mediated transactivation was further examined in the present study. Luciferase reporter (Fig. 2C), modified mammalian one-hybrid (Fig. 3B) and coimmunoprecipitation (Fig. 4B) assays using truncated mutants of TZF clearly demonstrated that a central portion (amino acids 512–663) of TZF is responsible for both binding to AR and repressing AR-mediated transactivation. Corepressor complexes containing N-CoR and SMRT are considered to recruit HDAC and then repress transcription (Jones and Shi, 2003). TZF also recruits endogenous HDAC2 and forms a complex with endogenous AR in the presence of DHT (Figs. 5C, 6B and 6C), and the specific HDAC inhibitor TSA completely prevented the transcriptional repression by TZF (Fig. 5A–C), suggesting that recruitment of HDAC2 into the AR/TZF complex is the major mechanism of the repression. Two of the truncated TZF mutants, namely TZF(1–663) and TZF(512–942), repressed AR-mediated transactivation much more strongly than full-length TZF, and a similar level of repression was observed for their common region, TZF(512–663). Based on these results, it may be speculated that the central portion (amino acids 512–663) is structurally positioned inside the TZF molecule, such that removal of the N- or C-terminal of the molecule may cause further exposure of the active domain, thereby resulting in a stronger interaction and repression of transactivation. TZF(512–663) does not contain a CoRNR motif (I/LXXII), which has been found in the corepressors N-CoR and SMRT and is considered to be sufficient for both their interactions with nuclear receptors and repression of transactivation (Webb et al., 2000; Hu et al., 2001). To examine whether TZF(512–663) contains some specific secondary structures, a protein structure prediction analysis was performed on this region (PredictProtein; Columbia University Bioinformatics Center, New York, NY). Although no regular secondary structures (helices, strands or coiled-coils) were found in this region, such a long region without any regular secondary structures is categorized into non-regular secondary structure (NORS), which indicates a structurally flexible region. NORS regions